

Investigate The Liquid Viscosity And Swirl Velocity On The Hollow Cone Spray Atomization

¹Fathollah Ommi, ²Seyed Askari Mahdavi, ³Ehsan Movahed Nejad, ⁴Koros Nekofar

¹Tarbiat Modares University, Engineering Faculty, Tehran, Iran.

²Mechanical Engineering, Tarbiat Modares University, Tehran, Iran.

³Islamic Azad University, Jolfa Branch, Jolfa, Iran.

⁴Islamic Azad University, Chaloos Branch, Civil department, Chaloos, Iran.

Abstract: A linear instability analysis of an annular liquid sheet emanating from an atomizer subjected to inner and outer air streams to investigate the liquid viscosity and swirl velocity on the maximum growth rate has been carried out. The dimensionless dispersion equation that governs the instability is derived. The dispersion equation solved by Numerical method. The result show that viscosity has negative and swirl velocity has positive effect on maximum growth rate and its corresponding unstable wave number that it produces the finest droplets.

Key words: Swirl Jet, Growth Rate, Linear Instability, Atomization, Primary Breakup.

INTRODUCTION

Fuel atomization is an important factor in the process of fuel injection which its development causes shortening of initial breakup of spray and the smaller diameter spray of droplets. The spinning atomization which produces hollow cone spray are used in big scales in gas turbine engines, industrial boilers, industrial and agricultural engines with gasoline direct injection (GDI) engines or spark ignition (DISI) (Senecal P.K., *et al.*, 1999). This atomization produces a spray as a thin fluid rotation due to radial play of the primary basis with medium pressure (Ashraf Ibrahim, 2006). Analysis and the breakup of the layer or fluid jet due to the growth of unstable waves are done at the common gas – liquid on aerodynamics contrast between gas and liquid.

This type of instability is called the Kolin Helmholtz instability (Panton R.L., 1995). Analytical and experimental studies have been done on the mechanism of atomization by individuals such as Rayleigh, Taylor, Weber, Anserg, Ritz, Brako, Ibrahim and other researchers (Rolf D.R., 1996).

Each of these individuals in their research with regard to boundary conditions and continuity and momentum equations of fluid and gas, they reached the equitation of maximum growth rate by simplifying the relationship between the waves. Actually wave maximum growth rate maximum wave frequency is the imaginary part in a number of critical waves which has occurred and caused breakup and fluid jet into ligaments and then it becomes droplet. Some persons in their studies have benefited of the rotational speed and fluid viscosity gas of inside and outside and some have given up these parameters.

For example, linear stability analysis of fluid layer under the influence of environmental gas, surface tension and viscosity of the fluid in the wave of development has been presented by Ritz and his colleagues (Senecal P.K.M *et al.*, 1999). Shen and Li (Shen J., *et al.*, 1996), Liao and his colleagues (Liao), by considering the fluid viscosity and the regardless the rotation of gas, they studied the unstable fluid layer rotating fluid. (Liao Y., *et al.*, 2001). Mehring and Sirignano did nonlinear analysis of instability with a rotating fluid and regardless of the gas. (Sirignano W.A., *et al.*, 2000). Ibrahim by applying non-viscosity fluid and gas spinning used linear method used for his analysis (Ibraim A.A., *et al.*, 2006). Usually those who consider the viscosity fluid effects, they do consider the speed flucations for simplicity of the analysis (Ibrahim A.A., *et al.*, 2006).

In the current article the atomization of a hollow cone spray slime under the rotating air flow fluctuations and non-sinusoidal slimy has been studied. And finally the effect of viscosity and rotational speed on fuel atomization has been discussed.

2. Linear Stability Analysis:

2.1. Model Assumptions:

In this modeling, the stability in an annular fluid layer rotating is considered about the slab exposed to air flow. The Gas – phase is assumed non – density and non–sticky.

Initial fluid velocity profiles, internal air and external air are respectively as $(U_i, 0, A_i/r)$ and $(U_o, 0, \Omega r)$ and that $A_o/r, \Omega r, A_i/r$ (m/s) is respectively the rotational speed of the fluid, internal and external gas and A_o, A_i (m^2/s) is the power of liquid and gas rotation. A liquid and gas velocity profile in outer vortex is freed as a swirl and the internal gas is assumed as a rotating solid object. Layer instability occurs due to the growth of unstable waves of the common level of gas – liquid. The growth rate of these unstable waves depends on fluid properties, nozzle geometry and the effect of each of the forces acting on the middle level, including viscosity, pressure, inertia and centrifugal force (the internal level).

Here has been tried to a linear instability analysis to determine maximum growth rates and unstable wave numbers. Figure 1 indicates a Schematic of an annular fluid layer where the liquid and gas axial and rotational velocities have been determined. R_i, R_o , are the inner and outer radius of the layers in a state without oscillation. ϕ , is the phase differences of the internal and external layers.

2.2. Linear Fluctuations Equations:

The slimy fluid flow equations in cylindrical coordinates are as follows:

Continuity Equation:

$$\frac{\partial U}{\partial x} + \frac{V}{r} + \frac{\partial V}{\partial r} + \frac{1}{r} \frac{\partial W}{\partial \theta} = 0 \tag{1}$$

Momentum Equations:

$$\frac{\partial U}{\partial t} + U \frac{\partial U}{\partial x} + V \frac{\partial U}{\partial r} + \frac{1}{r} W \frac{\partial U}{\partial \theta} = -\frac{1}{\rho} \frac{\partial P}{\partial x} + \nu \left(\frac{\partial^2 U}{\partial r^2} + \frac{1}{r} \frac{\partial U}{\partial r} + \frac{1}{r^2} \frac{\partial^2 U}{\partial \theta^2} + \frac{\partial^2 U}{\partial x^2} \right) \tag{2}$$

$$\frac{\partial V}{\partial t} + U \frac{\partial V}{\partial x} + V \frac{\partial V}{\partial r} + \frac{1}{r} W \frac{\partial V}{\partial \theta} - \frac{W^2}{r} = -\frac{1}{\rho} \frac{\partial P}{\partial r} + \nu \left(\frac{\partial^2 V}{\partial r^2} + \frac{1}{r} \frac{\partial V}{\partial r} + \frac{1}{r^2} \frac{\partial^2 V}{\partial \theta^2} - \frac{V}{r^2} - \frac{2}{r^2} \frac{\partial W}{\partial \theta} + \frac{\partial^2 V}{\partial x^2} \right) \tag{3}$$

$$\frac{\partial W}{\partial t} + U \frac{\partial W}{\partial x} + V \frac{\partial W}{\partial r} + \frac{1}{r} W \frac{\partial W}{\partial \theta} + \frac{VW}{r} = -\frac{1}{\rho r} \frac{\partial P}{\partial \theta} + \nu \left(\frac{\partial^2 W}{\partial r^2} + \frac{1}{r} \frac{\partial W}{\partial r} + \frac{1}{r^2} \frac{\partial^2 W}{\partial \theta^2} - \frac{W}{r^2} + \frac{2}{r^2} \frac{\partial V}{\partial \theta} + \frac{\partial^2 W}{\partial x^2} \right) \tag{4}$$

To obtain the linear oscillatory equations we assume the following. Can be seen that the terms include the average speed and pressure and marked with time fluctuating part are marked with Prim.

$$U = \bar{U} + u, \quad V = v, \quad W = \bar{W} + w, \quad p = \bar{P} + p' \tag{5}$$

Also assume that the fluctuations are as follows:

$$(u, v, w, p') = (\hat{u}(r), \hat{v}(r), \hat{w}(r), \hat{p}(r)) e^{i(kx+n\theta-\omega t)} \tag{6}$$

Oscillatory terms to the product of two component groups. The first component was marked \wedge with only a function of r and other parameters are included.

With the above assumptions apply linear equations of fluid can be written as follows:

Continuity Equation:

$$\frac{\partial u}{\partial x} + \frac{v}{r} + \frac{\partial v}{\partial r} + \frac{1}{r} \frac{\partial w}{\partial \theta} = 0 \tag{7}$$

Momentum Equations:

$$\frac{\partial u}{\partial t} + U_i \frac{\partial u}{\partial x} + \frac{A_i}{r^2} \frac{\partial u}{\partial \theta} = -\frac{1}{\rho_i} \frac{\partial p'}{\partial x} + \nu \left(\frac{\partial^2 u}{\partial r^2} + \frac{1}{r} \frac{\partial u}{\partial r} + \frac{1}{r^2} \frac{\partial^2 u}{\partial \theta^2} + \frac{\partial^2 u}{\partial x^2} \right) \tag{8}$$

$$\frac{\partial v}{\partial t} + U_i \frac{\partial v}{\partial x} + \frac{A_i}{r^2} \frac{\partial v}{\partial \theta} - \frac{2A_i w}{r^2} = -\frac{1}{\rho_i} \frac{\partial p'}{\partial r} + \nu \left(\frac{\partial^2 v}{\partial r^2} + \frac{1}{r} \frac{\partial v}{\partial r} + \frac{1}{r^2} \frac{\partial^2 v}{\partial \theta^2} - \frac{v}{r^2} - \frac{2}{r^2} \frac{\partial w}{\partial \theta} + \frac{\partial^2 v}{\partial x^2} \right) \tag{9}$$

$$\frac{\partial w}{\partial t} + U_i \frac{\partial w}{\partial x} + \frac{A_i}{r^2} \frac{\partial w}{\partial \theta} = -\frac{1}{\rho_i r} \frac{\partial p'}{\partial \theta} + \nu \left(\frac{\partial^2 w}{\partial r^2} + \frac{1}{r} \frac{\partial w}{\partial r} + \frac{1}{r^2} \frac{\partial^2 w}{\partial \theta^2} - \frac{w}{r^2} + \frac{2}{r^2} \frac{\partial v}{\partial \theta} + \frac{\partial^2 w}{\partial x^2} \right) \tag{10}$$

Linear equations by the internal and external gas are as follows:

Continuity Equation:

$$\frac{\partial u}{\partial x} + \frac{v}{r} + \frac{\partial v}{\partial r} + \frac{1}{r} \frac{\partial w}{\partial \theta} = 0 \tag{11}$$

Momentum Equations:

$$\frac{\partial u}{\partial t} + U_j \frac{\partial u}{\partial x} + \frac{W_j}{r} \frac{\partial u}{\partial \theta} = -\frac{1}{\rho_j} \frac{\partial p'_j}{\partial x} \tag{12}$$

$$\frac{\partial v}{\partial t} + U_j \frac{\partial v}{\partial x} + \frac{W_j}{r} \frac{\partial v}{\partial \theta} - \frac{2W_j w}{r} = -\frac{1}{\rho_j} \frac{\partial p'_j}{\partial r} \tag{13}$$

$$\frac{\partial w}{\partial t} + U_j \frac{\partial w}{\partial x} + \nu \frac{\partial W_j}{\partial r} + \frac{W_j}{r} \frac{\partial w}{\partial \theta} + \frac{W_j v}{r} = -\frac{1}{\rho_j r} \frac{\partial p'_j}{\partial \theta} \tag{14}$$

In the unstable analysis k is the wave number and n is real number, while the frequency of ω is a complex number. Maximum of the imaginary part ω represents maxim of the wave growth rate (Liao Y., *et al.*, 2000). Changing levels of volatility in internal and domestic joint surfaces is expressed by the following relations:

$$\eta_i(x, \theta, t) = \hat{\eta}_i e^{i(kx+n\theta-\omega t)+i\phi} \tag{15}$$

$$\eta_o(x, \theta, t) = \hat{\eta}_o e^{i(kx+n\theta-\omega t)} \tag{16}$$

To determine the effect of different forces, fluid properties and other geometric parameters, the following dimensionless parameters are introduced:

$$\begin{aligned}
 We_l &= \frac{\rho_l U_l^2 R_b}{\sigma}, \quad We_i = \frac{\rho_i U_i^2 R_b}{\sigma}, \quad We_o = \frac{\rho_o U_o^2 R_b}{\sigma}, \\
 We_s &= \frac{\rho_l W_l^2 R_b}{\sigma}, \quad We_{si} = \frac{\rho_i W_i^2 R_b}{\sigma}, \quad We_{so} = \frac{\rho_o W_o^2 R_b}{\sigma}, \\
 Re &= \frac{\rho_l U_l R_b}{\mu}, \quad g_i = \frac{\rho_i}{\rho_l}, \quad g_o = \frac{\rho_o}{\rho_l}, \quad \bar{k} = kR_b, \\
 \bar{\omega} &= \frac{\omega R_b}{U_l}, \quad \frac{U_i}{U_l} = \sqrt{\frac{We_i}{We_l} \frac{1}{g_i}}, \quad \frac{U_o}{U_l} = \sqrt{\frac{We_o}{We_l} \frac{1}{g_o}}, \\
 \frac{A_i}{U_l R_b} &= \sqrt{\frac{We_s}{We_l}}, \quad \frac{A_o}{U_l R_b} = \sqrt{\frac{We_{so}}{We_l} \frac{1}{g_o}}, \quad \frac{\Omega R_b}{U_l} = \sqrt{\frac{We_{si}}{We_l} \frac{1}{g_i}} \\
 , \bar{s} &= \left(\bar{k}^2 + \text{Re}(-i\bar{\omega} + i\bar{k}) \right)^{\frac{1}{2}}, \quad h = \frac{R_a}{R_b}
 \end{aligned}$$

Weber numbers for the fluid, the gas inside and outside states of axial and rotational speed were defined $Re, \bar{\omega}, \bar{k}, g_{i,o}, h$ are respectively Radius ratio, density ratio of gases to fluid, dimensionless wave number, dimensionless growth rate and Reynolds number of fluid flow.

2.3. Boundary Conditions:

Fluid kinematics boundary conditions can be written as follows:

$$v = \frac{\partial \eta_i}{\partial t} + \frac{1}{r^2} \frac{\partial \eta_i}{\partial \theta} \sqrt{\frac{We_s}{We_l}} + \frac{\partial \eta_i}{\partial x} \quad \text{at } r = h \tag{17}$$

$$v = \frac{\partial \eta_o}{\partial t} + \frac{1}{r^2} \frac{\partial \eta_o}{\partial \theta} \sqrt{\frac{We_s}{We_l}} + \frac{\partial \eta_o}{\partial x} \quad \text{at } r = 1 \tag{18}$$

Internal and external gas kinematic boundary conditions:

$$v_i = \frac{\partial \eta_i}{\partial t} + \frac{\partial \eta_i}{\partial \theta} \sqrt{\frac{We_{si}}{We_l} \frac{1}{g_i}} + \frac{\partial \eta_i}{\partial x} \sqrt{\frac{We_i}{We_l} \frac{1}{g_i}} \quad \text{at } r = h \tag{19}$$

$$v_o = \frac{\partial \eta_o}{\partial t} + \frac{1}{r^2} \frac{\partial \eta_o}{\partial \theta} \sqrt{\frac{We_{so}}{We_l} \frac{1}{g_o}} + \frac{\partial \eta_o}{\partial x} \sqrt{\frac{We_o}{We_l} \frac{1}{g_o}} \quad \text{at } r = 1 \tag{20}$$

Due to assuming the non – slimy of gas flow is non-axial and tangential directions, the viscous tension in jointed surface of fluid – gas is zero. This issue is expressed as follows:

$$\frac{\partial u}{\partial r} + \frac{\partial v}{\partial x} = 0 \quad \text{at } r = h, 1 \tag{21}$$

$$\frac{\partial w}{\partial r} - \frac{w}{r} + \frac{1}{r} \frac{\partial v}{\partial \theta} = 0 \quad \text{at } r = h, 1 \tag{22}$$

Regardless of the effects of fluctuations due to rotational speed, the equation 22 is used in calculations. Dynamic boundary conditions due to the balance of forces are expressed as follows:

$$p'_i - p'_i = \frac{1}{h^2 We_l} \left(\eta_i + \frac{\partial^2 \eta_i}{\partial \theta^2} + h^2 \frac{\partial^2 \eta_i}{\partial x^2} \right) + h \frac{We_{si}}{We_l} \eta_i - \frac{We_s}{We_l} \frac{\eta_i}{h^3} + \frac{2}{Re} \frac{\partial v}{\partial r} \quad \text{at } r = h \tag{23}$$

$$p'_l - p'_o = \frac{-1}{We_l} \left(\eta_o + \frac{\partial^2 \eta_o}{\partial \theta^2} + \frac{\partial^2 \eta_o}{\partial x^2} \right) + \frac{We_{so}}{We_l} \eta_o - \frac{We_s}{We_l} \eta_o + \frac{2}{Re} \frac{\partial v}{\partial r} \quad \text{at } r = 1 \quad (24)$$

2.4. Pressure Fluctuations In Fluid Layers:

Linear momentum and continuity equations and dimensionless fluid can be written with the assumptions stated in two slimy (index 2) and non – slimy (index 1) as follows:

Fluid equations in non – slimy mode:

$$\hat{u}_1(i\bar{k}) + \frac{d\hat{v}_1}{dr} + \frac{\hat{v}_1}{r} = 0 \quad (25)$$

$$\hat{u}_1(-i\bar{\omega} + i\bar{k}) = -i\bar{k}\hat{p} \quad (26)$$

$$\hat{v}_1(-i\bar{\omega} + i\bar{k}) = -\frac{d\hat{p}}{dr} \quad (27)$$

Fluid equations in the slimy state:

$$\hat{u}_2(i\bar{k}) + \frac{d\hat{v}_2}{dr} + \frac{\hat{v}_2}{r} = 0 \quad (28)$$

$$\hat{u}_2(-i\bar{\omega} + i\bar{k}) = \frac{1}{Re} \left(\frac{d^2 \hat{u}_2}{dr^2} + \frac{1}{r} \frac{d\hat{u}_2}{dr} - \frac{\hat{u}_2}{r^2} (\bar{k}^2 r^2) \right) \quad (29)$$

$$\hat{v}_2(-i\bar{\omega} + i\bar{k}) = \frac{1}{Re} \left(\frac{d^2 \hat{v}_2}{dr^2} + \frac{1}{r} \frac{d\hat{v}_2}{dr} - \frac{\hat{v}_2}{r^2} (\bar{k}^2 r^2 + 1) \right) \quad (30)$$

Fluid velocity terms are written as follows:

$$\hat{u} = \hat{u}_1 + \hat{u}_2, \hat{v} = \hat{v}_1 + \hat{v}_2 \quad (31)$$

By using the equations 26 and 27, the following relation is obtained:

$$\hat{v}_1 = \frac{1}{i\bar{k}} \frac{d\hat{u}_1}{dr} \quad (32)$$

By putting the relation 32 in the relation 25, the following equation is obtained:

$$\left(\frac{d^2 \hat{u}_1}{dr^2} + \frac{1}{r} \frac{d\hat{u}_1}{dr} - \frac{\hat{u}_1}{r^2} (\bar{k}^2 r^2) \right) = 0 \quad (33)$$

The above equation is a Bessel equation, which has a response to the following form:

$$\hat{u}_1 = C_1 I_0(\bar{k}r) + C_2 K_0(\bar{k}r) \quad (34)$$

By having the equations 34 and 32 and 26 we can reach the following two equations:

$$\hat{v}_1 = -i C_1 I_1(\bar{k}r) + i C_2 K_1(\bar{k}r) \quad (35)$$

$$\hat{p} = \frac{\bar{\omega} - \bar{k}}{\bar{k}} (C_1 I_0(\bar{k}r) + C_2 K_0(\bar{k}r)) \quad (36)$$

By applying the same technique on equations 28 to 30, finally the terms of speed are obtained as follows:

$$\hat{u} = C_1 I_0(\bar{k}r) + C_2 K_0(\bar{k}r) + C_3 I_0(\bar{s}r) + C_4 K_0(\bar{s}r) \tag{37}$$

$$\hat{v} = -i C_1 I_1(\bar{k}r) + i C_2 K_1(\bar{k}r) + C_5 I_1(\bar{s}r) + C_6 K_1(\bar{s}r) \tag{38}$$

Now by using fluid boundary conditions, i.e. equations 17 and 18 and 21, the coefficients of C_1 to C_6 , is calculated and by putting it in the equation 36 in the fluid fluctuation it will be written as following relation:

$$p'_i = \frac{\bar{\omega} - \bar{k}}{\bar{k}} \left(C_1 I_0(\bar{k}r) + C_2 K_0(\bar{k}r) \right) e^{i(\bar{k}x + n\theta - \bar{\omega}t)} \tag{39}$$

The above coefficients have been mentioned in the appendix.

2.5. Pressure Fluctuations In Gas Phase:

Continuity and momentum and dimensionless linear equations of gas phase can be written as follows:

$$\hat{u}(i\bar{k}) + \frac{d\hat{v}}{dr} + \frac{\hat{v}}{r} = 0 \tag{40}$$

$$\hat{u} \left(-i\bar{\omega} + i\bar{k} \sqrt{\frac{We_j}{We_i} \frac{1}{g_j}} \right) = -\frac{1}{g_j} i\bar{k}\hat{p} \tag{41}$$

$$\hat{v} \left(-i\bar{\omega} + i\bar{k} \sqrt{\frac{We_j}{We_i} \frac{1}{g_j}} \right) = -\frac{1}{g_j} \frac{d\hat{p}}{dr} \tag{42}$$

Fluctuations in gas pressure in the internal and external gas are calculated the same as fluid pressure fluctuations that mentioning the relevant operation is not done:

$$p'_i = \frac{g_i \left(\bar{\omega} - \bar{k} \sqrt{\frac{We_i}{We_l} \frac{1}{g_i}} \right)^2 \hat{\eta}_i e^{i\phi}}{\bar{k} I_1(\bar{k}h)} I_0(\bar{k}h) e^{i(\bar{k}x - \bar{\omega}t)} \tag{43}$$

$$p'_o = -\frac{g_o \left(\bar{\omega} - \bar{k} \sqrt{\frac{We_o}{We_l} \frac{1}{g_o}} \right)^2 \hat{\eta}_o}{\bar{k} K_1(\bar{k})} K_0(\bar{k}) e^{i(\bar{k}x - \bar{\omega}t)} \tag{44}$$

$K_n(v)$, $I_n(v)$ are the Bessel function of first and second type of the power n . By putting pressure fluctuations in equations 23 and 24 and omitting the joint factors from the dimensionless equation dimensionless nonlinear distribution forms are obtained as following [12]:

$$f(\bar{\omega}, \bar{k}, \bar{s}, g_i, g_o, Re, We_l, We_i, We_o, We_s, We_{si}, We_{so}, h) = 0 \tag{45}$$

The final equation is solved by using numerical methods and changing the input values on the roots i.e. the maxim of imaginary which indicates the fluctuation maxim growth rate and the duration of spray initial breakup is discussed.

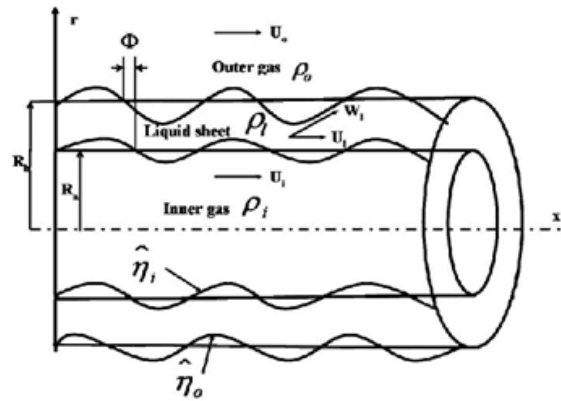


Fig. 1: Schematic form of rotating annular fluid layer.

3. Results:

Since the rotational speed fluctuation of w has not been considered in this article, so the effect of the average speed of W_i rotation is reviewed. By solving the distribution of dimensionless equation, the rotational speed of fluid effects can be demonstrated according to the following forms.

It is observed that the rotation and the rotational speed which is shown with the increase of the Weber number rotary fluid can increase the maximum growth rate. Figure 2 and 3 indicate the changes of the maximum growth rate in terms of number of wave modes with no rotation. Figures 4 and 5 show the maximum growth rate changes in a state of fluid rotating. The diagrams of the mentioned figures indicate that the fluid rotation and rotational speed has much influence on the maximum wave growth rate.

Also in the four figures of 2,3,4 and 5 it is observed that with increasing Reynolds number the maximum growth rate increases. As we know Reynolds number is the ratio of inertia the fluid viscosity. Therefore, increasing Reynolds number is equal to reduction of viscosity in the fixed speed and according to the diagrams; the reduction of viscosity is equal to the increase of maximum wave growth rate.

The more the maximum growth rate increases, the length and diameter of breakup of the droplet reduce and it causes improvement of combustion and reduction of pollutants and fuel consumption. Figure 6 shows the dual effect of fluid viscosity on wave maximum growth rate. It is observed that it has viscosity has reducing role in spinning Weber numbers and increasing role in higher Weber numbers higher in the maximum growth rate.

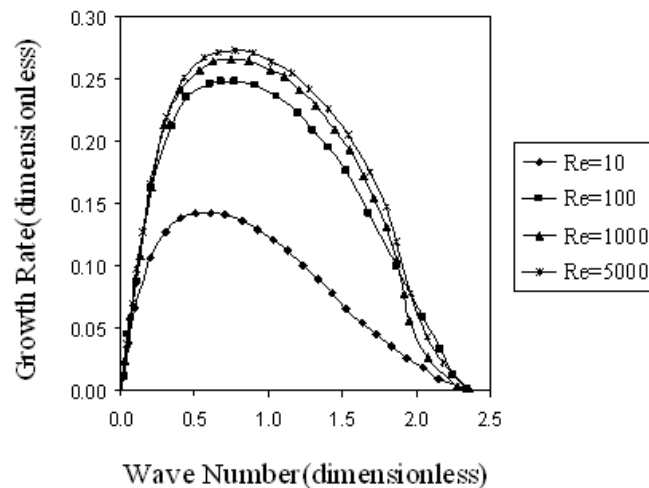


Fig. 2: The chart of wave maximum growth rate in the conditions. $We_l=1000$, $g_i=g_o=0.00123$, $h=0.9$

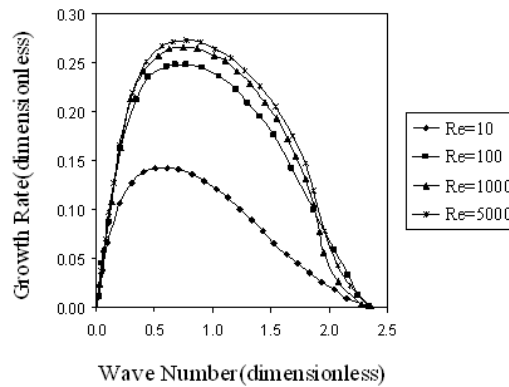


Fig. 3: The chart of wave maximum growth rate in the conditions. $Wel=10000$, $gi=go=0.00123$, $h=0.9$

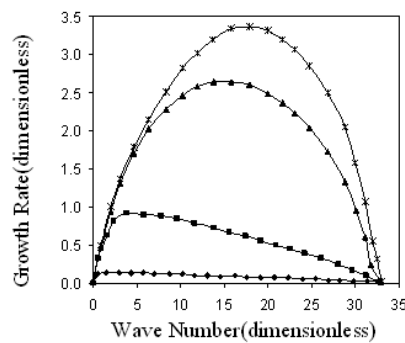


Fig. 4: The chart of wave maximum growth rate in the conditions. $Wel=Wes=1000$, $gi=go=0.00123$, $h=0.9$

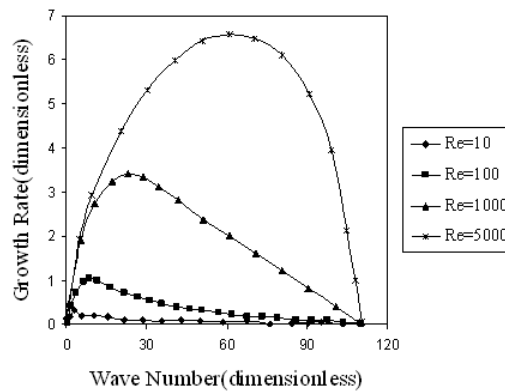


Fig. 5: The chart of wave maximum growth rate in the conditions. $Wel=Wes=10000$, $gi=go=0.00123$, $h=0.9$

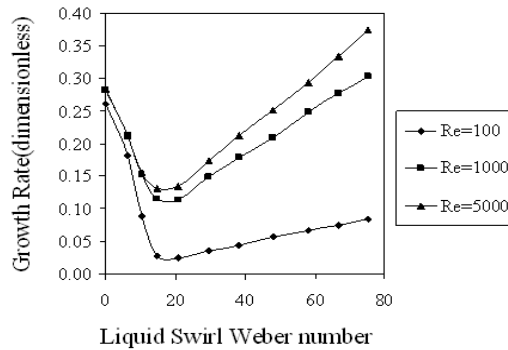


Fig. 6: The changes of wave maximum growth rate with viscosity and the fluid rotating Weber number in the conditions. $Wel=1000$, $gi=go=0.00123$, $h=0.9$

4. Conclusion And Summary:

The results show that increasing the rotational speed and reduction of the fluid viscosity are effective in increasing maxim growth rage and reduction of the initial breakup length and reduction of the droplet diameter and improvement of combustion and reduction of fuel consumption.

REFERENCES

Ashraf Ibrahim, 2006. Comprehensive Study of Internal Flow Field and Linear and Nonlinear Instability of an Annular Liquid Sheet Emanating from an Atomizer, 3231127.

Ibrahim, A.A., M.A Jog., S.M. Jeng, 2006. Effect of liquid swirl velocity profile on the instability of a swirling annular liquid sheet. *Atomization Spray*, 16: 237-263.

Ibrahim, A.A. and M.A. Jog, Cincinnati, Ohio, 2006. Effect of liquid and air swirl strength and relative rotational direction on the instability of an annular liquid sheet, *Acta Mechanica*, 186: 113-133.

Liao, Y., S.M. Jeng, M.A. Jog, M.A. Benjamin, 2001. Advanced sub – model for air blast atomizers. *J. Propulsion Power*, 17: 411-417.

Liao, Y., S.M. Jeng, M.A. Jog, M.A. Benjamin, 2000. Effect of air swirl profile on the instability of a viscous liquid jet. *J. Fluid Mech.*, 424: 1-20.

Liao, Y., Jeng, S.M., Jog, M.A. Benjamin, 2000. Instability of an annular liquid sheet surrounded by swirling airstreams. *AIAA J.*, 38: 453-460.

Liao, Y., S.M. Jeng, M.A. Jog, M.A. Benjamin, 1999. A Comprehensive model to predict simplex atomizer performance. *J. Engng. Gas Turbines Power*, 121: 285-294.

Panton, R.L., *Incompressible flow*, John Wiley and Sons, Inc., 1995.

Rolf, D., Reitz, 1996. *Spray Technology Short Course*, Wisconsin University, 7.

Senecal, P.K., D.P. Schmidt, I. Nouar, C.J. Rutland, R.D. Reitz, M.L. Corradini, 1999. “Modeling High-Speed Viscous Liquid Sheet Atomization”, *Int. J. of Multiphase Flow*, 25: 1073-1097.

Shen, J., X. Li, 1996. Instability of an annular viscous liquid jet. *Acta Mech.*, 114: 167-183.

Sirignano, W.A., C. Mehring, 2000. Review of theory of distortion and disintegration of liquid streams. *Prog. Energy Combustion Sci.*, 26: 609-655.

Appendix:

$$C_1 = \frac{-(\bar{k}^3 \hat{\eta}_i e^{i\phi} K_1(\bar{k}h) - \bar{k}^2 \bar{\omega} \hat{\eta}_i e^{i\phi} K_1(\bar{k}h) + \bar{k} \bar{s}^2 \hat{\eta}_i e^{i\phi} K_1(\bar{k}h) - \bar{s}^2 \bar{\omega} \hat{\eta}_i e^{i\phi} K_1(\bar{k}h))}{(-K_1(\bar{k}h)I_1(\bar{k}) + I_1(\bar{k}h)K_1(\bar{k}))(\bar{k}^2 - \bar{s}^2)} \tag{46}$$

$$\frac{(\bar{s}^2 \bar{\omega} \hat{\eta}_o K_1(\bar{k}) - \bar{k}^3 \hat{\eta}_o K_1(\bar{k}) + \bar{k}^2 \bar{\omega} \hat{\eta}_o K_1(\bar{k}) - \bar{s}^2 \hat{\eta}_o \bar{k} K_1(\bar{k}))}{(-K_1(\bar{k}h)I_1(\bar{k}) + I_1(\bar{k}h)K_1(\bar{k}))(\bar{k}^2 - \bar{s}^2)}$$

$$C_2 = \frac{-(-\bar{k}^3 \hat{\eta}_o I_1(\bar{k}) + \bar{k}^3 \hat{\eta}_i e^{i\phi} I_1(\bar{k}h) + \bar{k}^2 \bar{\omega} \hat{\eta}_o I_1(\bar{k}) - \bar{k}^2 \bar{\omega} \hat{\eta}_i e^{i\phi} I_1(\bar{k}h))}{(-K_1(\bar{k}h)I_1(\bar{k}) + I_1(\bar{k}h)K_1(\bar{k}))(\bar{k}^2 - \bar{s}^2)} \tag{47}$$

$$-\left(\frac{-\bar{s}^2 \bar{k} \hat{\eta}_o I_1(\bar{k}) + \bar{k} \hat{\eta}_i \bar{s}^2 e^{i\phi} I_1(\bar{k}h) + \bar{s}^2 \bar{\omega} \hat{\eta}_o I_1(\bar{k}) - \bar{s}^2 \bar{\omega} \hat{\eta}_i e^{i\phi} I_1(\bar{k}h)}{(-K_1(\bar{k}h)I_1(\bar{k}) + I_1(\bar{k}h)K_1(\bar{k}))(\bar{k}^2 - \bar{s}^2)} \right)$$

$$C_3 = \frac{2\bar{s}^2 \bar{k} (-\bar{k} \hat{\eta}_o K_1(\bar{s}) + \bar{k} \hat{\eta}_i e^{i\phi} K_1(\bar{s}h) - \hat{\eta}_i e^{i\phi} \bar{\omega} K_1(\bar{s}h) + \hat{\eta}_o \bar{\omega} K_1(\bar{s}))}{(\bar{k}^2 - \bar{s}^2)(-I_1(\bar{s})K_1(\bar{s}h) + K_1(\bar{s})I_1(\bar{s}h))} \tag{48}$$

$$C_4 = \frac{-2\bar{s}^2\bar{k}(\bar{k}\hat{\eta}_i e^{i\phi} I_1(\bar{s}h) - \bar{\omega}\hat{\eta}_i e^{i\phi} I_1(\bar{s}h) - \hat{\eta}_o \bar{k} I_1(\bar{s}) + \hat{\eta}_o \bar{\omega} I_1(\bar{s}))}{-\bar{k}^2 I_1(\bar{s}) K_1(\bar{s}h) + \bar{s}^2 I_1(\bar{s}) K_1(\bar{s}h) + \bar{k}^2 K_1(\bar{s}) I_1(\bar{s}h) - \bar{s}^2 K_1(\bar{s}) I_1(\bar{s}h)} \quad (49)$$

$$C_5 = \frac{-2i\bar{k}^2(-\bar{k}\hat{\eta}_o K_1(\bar{s}) + \bar{k}\hat{\eta}_i e^{i\phi} K_1(\bar{s}h) - \hat{\eta}_i e^{i\phi} \bar{\omega} K_1(\bar{s}h) + \hat{\eta}_o \bar{\omega} K_1(\bar{s}))}{(\bar{k}^2 - \bar{s}^2)(-I_1(\bar{s}) K_1(\bar{s}h) + K_1(\bar{s}) I_1(\bar{s}h))} \quad (50)$$

$$C_6 = \frac{2i\bar{k}^2(\bar{k}\hat{\eta}_i e^{i\phi} I_1(\bar{s}h) - \bar{\omega}\hat{\eta}_i e^{i\phi} I_1(\bar{s}h) - \hat{\eta}_o \bar{k} I_1(\bar{s}) + \hat{\eta}_o \bar{\omega} I_1(\bar{s}))}{-\bar{k}^2 I_1(\bar{s}) K_1(\bar{s}h) + \bar{s}^2 I_1(\bar{s}) K_1(\bar{s}h) + \bar{k}^2 K_1(\bar{s}) I_1(\bar{s}h) - \bar{s}^2 K_1(\bar{s}) I_1(\bar{s}h)} \quad (51)$$